Langmuir
Article
pubs.acs.org/Langmuir

Tribology Study of Reduced Graphene Oxide Sheets on Silicon Substrate Synthesized via Covalent Assembly

Junfei Ou,[†,‡] Jinqing Wang,*[,†] Sheng Liu,[†,‡] Bo Mu,[†] Junfang Ren,[†] Honggang Wang,[†] and Shengrong Yang*[,†]

[†]*State Key Laboratory of Solid Lubrication, Lanzhou Institute of Chemical Physics, Chinese Academy of Sciences, Lanzhou 730000, People's Republic of China, and* [‡]*Graduate University of Chinese Academy of Sciences, Beijing 100080, People's Republic of China*

Received December 10, 2009. Revised Manuscript Received September 7, 2010

Reduced graphene oxide (RGO) sheets were covalently assembled onto silicon wafers via a multistep route based on the chemical adsorption and thermal reduction of graphene oxide (GO). The formation and microstructure of RGO were analyzed by X-ray photoelectron spectroscopy (XPS), attenuated total reflectance Fourier transform infrared (ATR-FTIR) spectroscopy, Raman spectroscopy, and water contact angle (WCA) measurements. Characterization by atomic force microscopy (AFM) was performed to evaluate the morphology and microtribological behaviors of the samples. Macrotribological performance was tested on a ball-on-plate tribometer. Results show that the assembled RGO possesses good friction reduction and antiwear ability, properties ascribed to its intrinsic structure, that is, the covalent bonding to the substrate and self-lubricating property of RGO.

1. Introduction

Graphene, a 2D atomic thin layer of carbon nanostructure, has emerged as an ideal candidate for the basic building block of future micro- and nanoelectromechanical systems (MEMS/NEMS) because of its favorable characteristics, such as outstanding thermal conductivity,[1] novel electronic properties,[2] and excellent mechanical behaviors.[3] However, the realization of its potential has been severely restricted by the difficulty of obtaining a stable graphene structure on device surfaces by common solution process. This difficulty is attributed to the lack of function groups in graphene. Fortunately, the existence of abundant oxygenous groups in graphene oxide (GO) molecules makes it feasible to assemble the GO microstructure onto a substrate via certain interactions.[4−7] Moreover, reduced GO (RGO) can be easily obtained by thermal treatment.[8] On the basis of these features, we covalently assembled stable RGO sheets onto the surface of a silicon wafer through a multistep route. First, a 3-aminopropyl triethoxysilane self-assembled monolayer (coded APTES-SAM) was prepared on the silicon wafer via a self-assembly process. GO was then grafted onto a silicon substrate covered with APTES-SAM through chemical reactions between the oxygenous and amine groups. Finally, the formed GO was converted into RGO by thermal reduction for its simplicity and efficiency. The as-obtained sample was coded APTES-RGO.[8]

Aside from its well-known merits mentioned above, RGO is also expected to have good tribological performance for its derivation from self-lubricating graphite, which exhibits low friction and wear rate with no requirements for additional lubricants.[9,10] However, graphite is not a suitable candidate as lubricant for MEMS/NEMS because of the dimension mismatch. Specifically, the separations between MEMS/NEMS can range from 1 μm/100 nm to contact.[11] Correspondingly, the potential lubricant film should be nanoscaled. However, the typical scale of graphite sheet is micrometer or millimeter scaled. Therefore, a graphene/RGO sheet, which has a thickness of several nanometers, will be an ideal choice as lubricant film on nanoscale because of its derivation from graphite. Moreover, graphene/RGO possesses novel thermal, electronic, and mechanical properties. Therefore, effective usage of graphene/RGO as lubricant in MEMS/NEMS may depend on its nanoscale thickness and multipurpose applications. To date, the friction reduction and wear resistance of RGO have been rarely referred to. In this study, the tribological behaviors of the assembled APTES-RGO are investigated, as we aim to develop a simple and feasible route for fabricating multifunctional graphene coating materials. It is anticipated that these materials may find broad potential applications in MEMS/NEMS, not only for their excellent electronic and mechanical properties but also for their potential friction reduction and antistiction performance.

2. Experimental Section

2.1. Materials. Expandable graphite was obtained from Qingdao Hensen Graphite. Highly oriented pyrolytic graphite (HOPG) was supplied by SPI Supplies. P-type polished single-crystal silicon (111) wafers were purchased from GRINM Semiconductor Materials. 3-Aminopropyl triethoxysilane (APTES, 99%) was purchased from Acros Organics. Other reagents were of analytical grade and used as received. Ultrapure water (> 18 MΩ·cm) was used throughout the experiment.

*To whom correspondence should be addressed. Tel: +86-931-4968076. Fax: +86-931-8277088. E-mail: jqwang@licp.cas.cn (J.W.); sryang@licp.cas.cn (S.Y.).

(1) Du, X.; Skachko, I.; Barker, A.; Andrei, E. Y. *Nat. Nanotechnol.* **2008**, *3*, 491–495.
(2) Areshkin, D. A.; Gunlycke, D.; White, C. T. *Nano Lett.* **2007**, *7*, 204–210.
(3) Lee, C.; Wei, X.; Kysar, J. W.; Hone, J. *Science* **2008**, *321*, 385–388.
(4) Bourlinos, A. B.; Gournis, D.; Petridis, D.; Szabó, T.; Szeri, A.; Dékány, I. *Langmuir* **2003**, *19*, 6050–6055.
(5) Yang, H.; Li, F.; Shan, C.; Han, D.; Zhang, Q.; Niu, L.; Ivaska, A. *J. Mater. Chem.* **2009**, *19*, 4632–4638.
(6) Wei, Z.; Barlow, D. E.; Sheehan, P. E. *Nano Lett.* **2008**, *8*, 3141–3145.
(7) Kim, Y. K.; Min, D. H. *Langmuir* **2009**, *25*, 11302–11306.
(8) Kang, H.; Kulkarni, A.; Stankovich, S.; Ruoff, R. S.; Baik, S. *Carbon* **2009**, *47*, 1520–1525.
(9) Teer, D. G. *Wear* **2001**, *251*, 1068–1074.
(10) Pleskachevsky, Y. M.; Kovtun, V. A.; Kirpichenko, Y. E. *Wear* **1997**, *203*, 679–684.
(11) Chandross, M.; Lorenz, C. D.; Grest, G. S.; Stevens, M. J.; Webb, E. B. *JOM* **2005**, *57*, 55–61.

2.2. Preparation of GO Colloid Solution. Expandable graphite was first heated at 1050 °C in air for 15 s. The heat-treated expandable graphite powder (1 g) was then added to 98% H_2SO_4 (23 mL) in an ice bath with stirring, and $KMnO_4$ (3 g) was subsequently added slowly. The mixture was kept at 35 °C in a water bath for 30 min. Ultrapure water (46 mL) was gradually added, and the mixture was immersed in ice−water. After 15 min, the mixture was further treated with ultrapure water (140 mL) and 30% H_2O_2 solution (12.5 mL). The obtained mixture was first washed with ultrapure water until a pH level of 7 was reached and was then dialyzed with stirring until SO_4^{2-} anions could no longer be detected by the $BaCl_2$ solution (1 M). A diluted GO colloid solution with a concentration of 0.4 mg·mL^{-1} was employed in the succeeding process.

2.3. Assembly and Thermal Reduction of GO. Prior to assembly, silicon wafers were cleaned and hydroxylated in a piranha solution (a mixture of 7:3 (v/v) 98% H_2SO_4 and 30% H_2O_2) at 90 °C for 30 min. After being thoroughly rinsed with ultrapure water and blown dry with N_2, the silicon wafers were immersed in a freshly prepared APTES solution (5 mM, the solvent is a mixture of acetone and water, with a volume ratio of 5:1) for 30 min. Then, the wafers were taken out and sonicated in ultrapure water, generating the desired APTES-SAM thereon. Subsequently, the APTES-SAM-covered silicon substrate was kept in a GO aqueous solution at 80 °C for 12 h, then ultrasonically cleaned in ultrapure water and blown dry with N_2. The obtained sample was coded APTES-GO. Finally, APTES-GO was thermally reduced at 200 °C for 2 h at a heating rate of 1 °C·min^{-1} under an argon atmosphere.[8] The obtained sample was defined as APTES-RGO. For comparison, we prepared GO/RGO on a bare silicon substrate by adopting the same procedure in which the deposition of APTES-SAM was omitted.

To clarify further the reactions between APTES and GO molecules, APTES-GO and APTES-RGO powders were prepared according to the following procedure. Fourier transform infrared (FTIR) spectra were subsequently recorded. First, 20 mL of aqueous solution containing GO (0.2 mg/mL) and APTES (25 μL/mL) was kept at 80 °C for 12 h. The resultant colloid solution was then washed with ultrapure water and vacuum-filtered five times. The APTES-GO powder was vacuum-dried at 40 °C for 24 h. Finally, the APTES-GO powder was thermally reduced at 200 °C for 2 h at a heating rate of 1 °C·min^{-1} under an argon atmosphere to obtain the APTES-RGO powder.

2.4. Characterization. FTIR spectra of the prepared powder samples were recorded with an IFS 66 V/S FTIR spectrometer (Bruker, Germany). For the film samples, attenuated total reflectance Fourier transform infrared (ATR-FTIR) spectra were recorded with the same spectrometer using a Harrick Scientific horizontal reflection Ge-attenuated total reflection accessory (GATR, incidence angle 65°). The samples were placed in contact with the flat surface of a semispherical Ge crystal as the optical element. The spectrum was collected for 32 scans with a resolution of 4 cm^{-1}, and the background was collected using the accessory in the absence of the samples. To eliminate the effect of H_2O and CO_2, the pressure in the sample chamber and optical chamber was kept below 6.0×10^{-4} MPa.

Raman spectra (Lab RAMHR800, Horiba, Hobin Yvon, France, 532 nm laser excitation) were employed to characterize the microstructure of the samples.

The water contact angle (WCA) of different samples was determined using a DSA100 contact angle meter (Krüss, Germany). The averaged values of at least five repeat measurements for each sample were obtained.

X-ray photoelectron spectroscopy (XPS, PHI-5702, Physical Electronics) was performed using a monochromated Al Kα irradiation. The chamber pressure was $\sim 3 \times 10^{-8}$ Torr under testing conditions. Peak deconvolution and quantification of elements were accomplished using Origin 7.0.

The surface morphologies of different samples were observed by a Nanoscope IIIa multimode atomic force microscope (AFM, Veeco) in tapping mode. The microtribological properties of different film samples were measured using the same AFM in contact mode. Triangular silicon nitride cantilevers with a normal force constant of 2 N·m^{-1} were employed for AFM measurements. No attempt was made to calibrate the torsional force constant, and the same cantilever was applied in all measurements. The output voltages were directly used as the relative frictional force. A series of measurements of friction-load relationship was conducted from friction loops obtained from at least five separate locations on each sample surface. To obtain the adhesive force between the AFM tip and the film surface, the force−distance curve was recorded on a CSPM 4000 AFM (Being Nano-Instrument, China). The pull-off force was considered to be the adhesive force. All experiments were carried out under ambient conditions of 25 °C and 30% relative humidity.

Macrotribological tests were run on a UMT-2MT tribometer (CETR) in a ball-on-plate contact configuration. Commercially available steel balls (φ = 3 mm, announced mean roughness = 0.02 μm) were used as the stationary upper counterparts, whereas the lower tested samples were mounted onto the flat base and driven to slide reciprocally at a distance of 0.5 cm. The friction coefficient-versus-time curves were recorded automatically. At least three repeat measurements were performed for each frictional pair. The friction coefficient and antiwear life were measured at a relative error of ±10 and ±5%, respectively.

3. Results and Discussion

3.1. Assembly and Reduction of APTES-GO. GO is a graphite derivative with covalently attached oxygen-containing groups (such as epoxy, carboxyl, and hydroxyl groups; Figure 1a) generated in synthesis.[4,12,13] The existence of abundant polar oxygenous groups enables the satisfactory dispersion of GO in the aqueous solution (Figure 1b) and further modification through certain chemical reactions.[14] As reported by Niu et al., the epoxy group of GO can react with the amine group of APTES molecules.[5] Moreover, the carboxyl group is also expected to induce amidation between GO and amine-containing APTES.[15−20] Taking advantage of these potential reactions, we chemically bonded GO onto the APTES-SAM-covered silicon substrate. The formation and characterization of the APTES-SAM transition layer have been reported in our previous studies.[18,21] As experimental results indicate, APTES-SAM terminated with the amine group is formed successfully on the hydroxylated silicon wafer.

To demonstrate the actual occurrence of chemical reactions between APTES and GO, FTIR spectra of different samples were recorded (Figure 2). As shown in Figure 2a, the GO powder sample exhibits the following characteristic features: O−H stretching of the C−OH at 3415 cm^{-1}, C=O stretching of the −COOH at 1725 cm^{-1}, O−H bending of C−OH at 1618 cm^{-1}, O−H vibration of the C−OH groups at 1385 cm^{-1}, C−O vibration of the C−OH at 1260 cm^{-1}, and epoxy vibration at 1050 and

(12) Dékány, I.; Krüger-Grasser, R.; Weiss, A. *Colloid Polym. Sci.* **1998**, *276*, 570–576.
(13) Lerf, A.; He, H.; Forster, M.; Klinowski, J. *J. Phys. Chem. B* **1998**, *102*, 4477–4482.
(14) Dreyer, D. R.; Park, S.; Bielawski, C. W.; Ruoff, R. S. *Chem. Soc. Rev.* **2010**, *39*, 228–240.
(15) Song, S. Y.; Ren, S. L.; Wang, J. Q.; Yang, S. R.; Zhang, J. Y. *Langmuir* **2006**, *22*, 6010–6015.
(16) Song, S. Y.; Zhou, J. F.; Qu, M. N.; Yang, S. R.; Zhang, J. Y. *Langmuir* **2008**, *24*, 105–109.
(17) Song, S. Y.; Chu, R. Q.; Zhou, J. F.; Yang, S. R.; Zhang, J. Y. *J. Phys. Chem. C* **2008**, *112*, 3805–3810.
(18) Ren, S. L.; Yang, S. R.; Zhao, Y. P. *Langmuir* **2003**, *19*, 2763–2767.
(19) Ren, S. L.; Yang, S. R.; Zhao, Y. P.; Yu, T. X.; Xiao, X. D. *Surf. Sci.* **2003**, *546*, 64–74.
(20) Ren, S. L.; Yang, S. R.; Wang, J. Q.; Liu, W. M.; Zhao, Y. P. *Chem. Mater.* **2004**, *16*, 428–434.
(21) Ou, J. F.; Wang, J. Q; Liu, S.; Zhou, J. F; Ren, S. L; Yang, S. R. *Appl. Surf. Sci.* **2009**, *256*, 894–899.

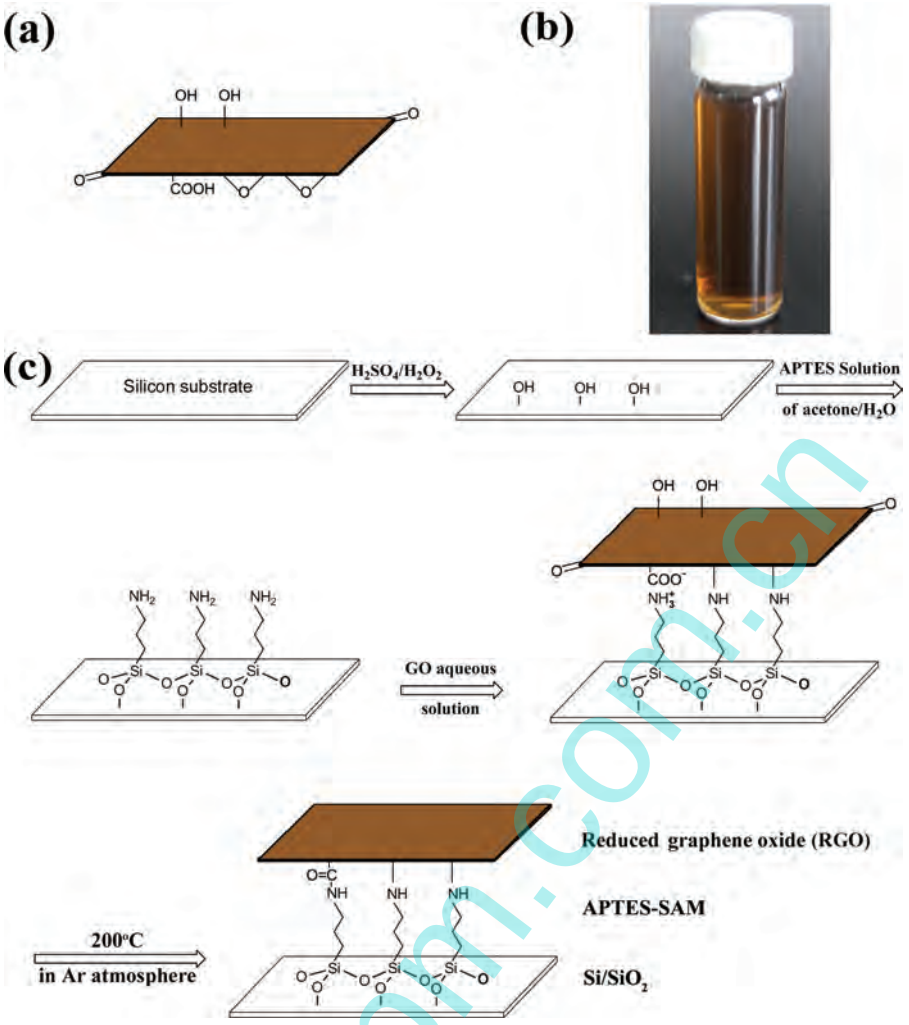

Figure 1. (a) Proposed chemical structure of GO. (b) Photo of aqueous dispersion (0.4 mg·mL^{-1}) of GO. (c) Proposed schematic view for the assembly and thermal reduction of APTES-GO on a silicon wafer.

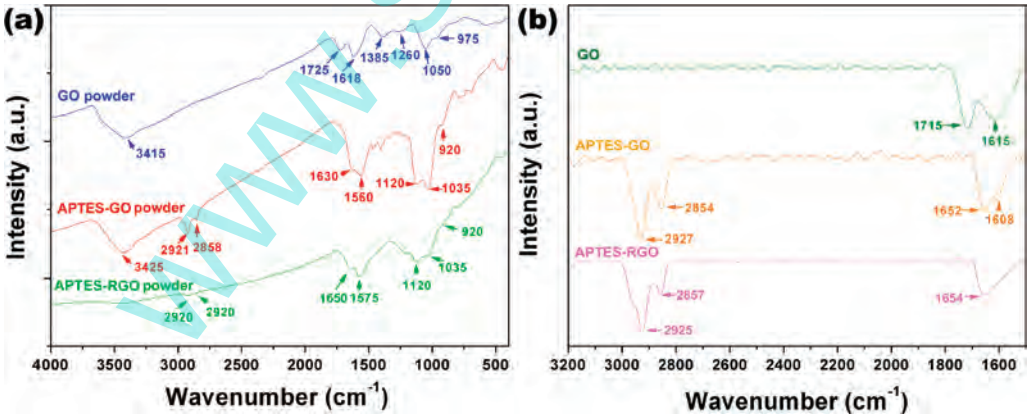

Figure 2. (a) FTIR and (b) ATR-FTIR spectra of different samples.

975 cm^{-1}.[5,22–26] After reacting with APTES, the characteristic bands of epoxy groups (i.e., 1050 and 975 cm^{-1}) vanish, and the typical signals of Si−O−Si (1035 and 920 cm^{-1}), which are ascribed to the hydroxylation of APTES molecules in the aqueous solution, arise.[27] Therefore, it is rational to deduce that the epoxy group experiences ring-opening under the attack of the amine group of APTES.[5] The doublet at 2921/2858 cm^{-1} and peak at

(22) Jeong, H. K.; Lee, Y. P.; Jin, M. H.; Kim, E. S.; Bae, J. J. *Chem. Phys. Lett.* **2009**, *470*, 255–258.
(23) Titelman, G.. I.; Gelman, V.; Bron, S.; Khalfin, R. L.; Cohen, Y.; Bianco-Peled, H. *Carbon* **2005**, *43*, 641–649.
(24) Szabó, T.; Berkesi, O.; Dékány, I. *Carbon* **2005**, *43*, 3181–3194.
(25) Shan, C. S.; Yang, H. F.; Han, D. X.; Zhang, Q. X.; Ivaska, A.; Niu, L. *Langmuir* **2009**, *25*, 12030–12033.
(26) Xu, C.; Wang, X.; Yang, L. C.; Wu, Y. P. *J. Solid State Chem.* **2009**, *182*, 2486–2490.
(27) Vandenberg, E. T.; Bertilsson, L.; Liedberg, B.; Uvdal, K.; Erlandsson, R.; Elwing, H.; Lundström, I. *J. Colloid Interface Sci.* **1991**, *147*, 103–118.

Table 1. WCA for Various Samples

samples	Si/SiO_2	APTES-SAM	APTES-GO	APTES-RGO	HOPG	RGO
WCA/deg	~0	48.0 ± 1.6	40.2 ± 2.0	85.5 ± 1.3	91.0 ± 2.5	82.4 ± 1.8

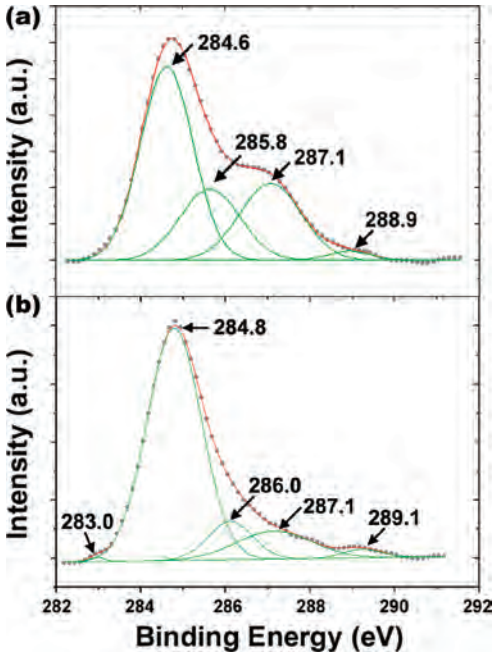

Figure 3. XPS spectra of C 1s for GO on bare Si substrate (a) before and (b) after thermal reduction.

1120 cm^{-1} correspond to CH_2 and C−N of the alkyl chains of APTES moieties in APTES-GO, respectively.[5] Moreover, the disappearance of C═O stretching in −COOH (i.e., 1725 cm^{-1}) and the newly emerged bands at 1630/1560 cm^{-1} suggest that the carboxyl groups undergo a great structural change. Considering the absence of a coupling agent such as 1-ethyl-3-(3-dimethylaminopropyl)-carbodiimide (EDC) or *N*,*N*′-dicyclohexylcarbodiimide (DCC), the amido linkages are not expected to be generated.[14] A rational explanation for the disappearance of carboxylic IR modes may be the formation of zwitterionic $COO^-NH_3^+$ linkages. It is generally believed that high temperature is in favor of producing amido linkage between carboxylic and amine groups.[28] So, the CO-NH linkage (1650/1575 cm^{-1}) is supposed to be formed during preparation of the sample of APTES-RGO powder at the thermal treatment temperature of 200 °C. Therefore, it is concluded that the amine group of APTES can react with the epoxy and carboxyl groups via nucleophilic substitution and amidation, respectively. ATR-FTIR spectra of different film samples are depicted in Figure 2b. For GO on the bare silicon substrate, two peaks located at 1715 and 1615 cm^{-1} can be ascribed to the C═O stretching of −COOH and O−H bending of C−OH, respectively. For film samples of APTES-GO and APTES-RGO, the peak located at 1652/1654 cm^{-1} can be ascribed to the C═O stretching of the zwitterionic $COO^-NH_3^+$ and amido linkage, respectively. Nevertheless, the lower wavenumber spectrum, which may involve the signals of the epoxy and Si−O−Si group, is not given for the low signal-to-noise of ATR-FTIR.

WCA measurement is a simple, useful, and sensitive tool for gaining insight into surface chemical components. As depicted in Table 1, the hydroxylated silicon substrate exhibits a low WCA

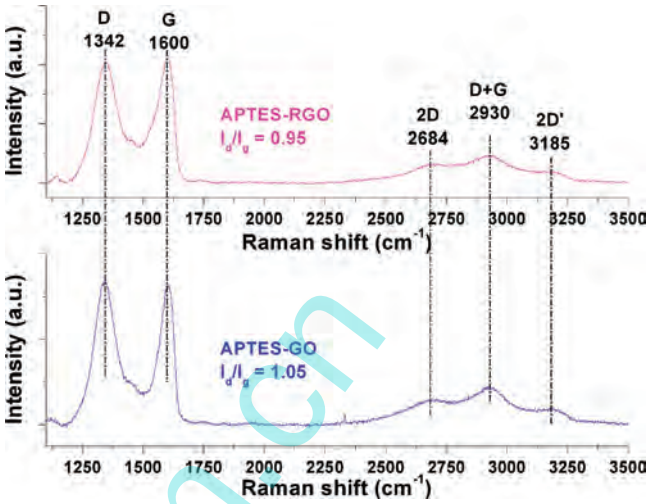

Figure 4. Raman spectra of APTES-GO and APTES-RGO.

of ~0°, which is attributed to the abundant surface hydroxyl groups generated in the piranha solution. APTES-SAM and APTES-GO are also hydrophilic, with WCAs of about 48 and 40.2°. The hydrophilicities are attributed to the outer amine groups of APTES-SAM and the oxygenous groups on APTES-GO. Upon the thermal reduction of APTES-GO, WCA increases to 85.5°. The sharp increase in WCA suggests that the oxygenous groups have been thermally removed. Furthermore, deoxygenation can be substantiated directly by XPS analysis. As shown in Figure 3a, XPS spectrum of C 1s for GO can be deconvoluted into four Gaussian peaks, which are typical signals of C−C (284.6 eV), C−O (hydroxyl and epoxy groups, 285.8 eV), C═O (287.1 eV), and O−C═O (288.9 eV).[29] Upon thermal reduction, these peaks remain observable. However, the content of oxygenated carbon decreases from 47.5 to 24.5%. Moreover, an unexpected weak signal at 283.0 eV emerged. According to ref 30, the origin of the peak at 283.0 eV is generally believed to result from the carbide. Namely, this weak peak may be attributed to the Si−C, which may exist between the bare silicon substrate and RGO sheets. However, there is no other solid and direct evidence to prove the occurrence of the Si−C bonding, and the forming mechanism is also not clear. Therefore, further investigation is necessary and in progress.

Raman spectra of APTES-GO and APTES-RGO are shown in Figure 4. The curves display two prominent peaks at 1342 and 1600 cm^{-1} corresponding to the D and G modes, respectively. 2D, D+G, and 2D′ peaks are also observed.[31] The G mode is related to the vibration of sp^2-hybridized carbon, whereas the D mode corresponds to the sp^3-hybridized carbon and defects associated with vacancies and grain boundaries in GO/RGO.[8] Therefore, the intensity ratio of I_d/I_g is related to the microstructure of GO/RGO. The heat reduction would cause microstructure change in

(28) Mo, Y. F.; Zhu, M.; Bai, M. W. *Colloids Surf., A* **2008**, *322*, 170–176.

(29) Yang, D. X.; Velamakanni, A.; Bozoklu, G.; Park, S.; Stoller, M.; Piner, R. D.; Stankovich, S.; Jung, I.; Field, D. A.; Ventrice, C. A., Jr.; Ruoff, R. S. *Carbon* **2009**, *47*, 145–152.

(30) Moulder, J.; Stickle, W. F.; Sobol, P. E.; Bomben, K. D. *Handbook of X-ray Photoelectron Spectroscopy*, 2nd ed.; Perkin Elmer Corporation: Eden Prairie, MN, 1992.

(31) Su, C. -Y.; Xu, Y.; Zhang, W.; Zhao, J.; Tang, X.; Tsai, C.-H.; Li, L.-J. *Chem. Mater.* **2009**, *21*, 5674–5680.

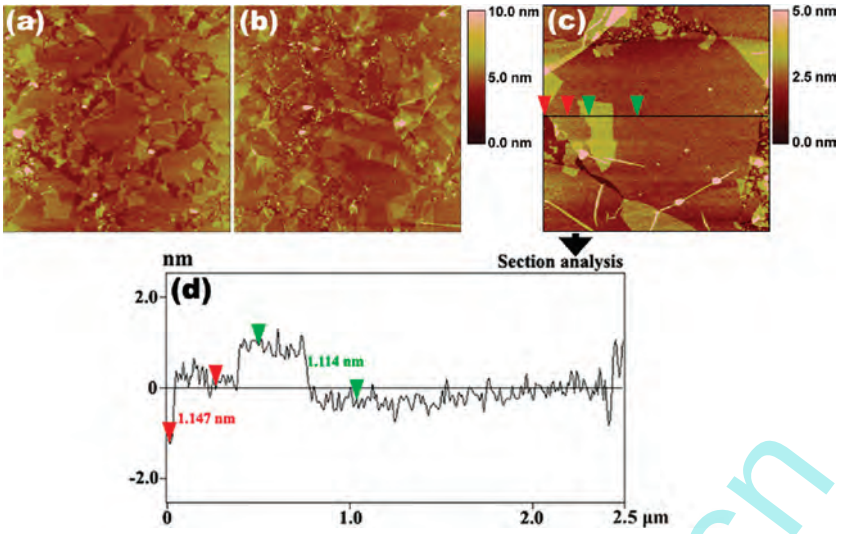

Figure 5. AFM images of (a) APTES-GO and (b,c) APTES-RGO and (d) the corresponding section analysis. The scanning area for a−c is 5 × 5, 5 × 5, and 2.5 × 2.5 μm^2, respectively. The Z range for a−c is 10, 10, and 5 nm, respectively.

GO. On one hand, as XPS results show, most oxygenous groups are eliminated and sp^3-hybridized carbon is converted to sp^2-hybridized carbon. On the other hand, under thermal treatment, GO sheets would split into smaller domains, and more defects are supposed to be generated. However, as AFM images depict (Figure 5a,b), the fragmentation of GO sheets is controlled to a certain degree because of the relatively low heat-treatment temperature of 200 °C. Therefore, upon thermal reduction, deoxygenation takes main responsibility for the decreased intensity ratio of I_d/I_g. Using a relatively low reduction temperature of 180 °C, the similar result has also been observed by Loh et al.[32]

To obtain more precise information on the surface microstructure, we observed the surface morphology of APTES-GO/APTES-RGO by AFM. As shown in Figure 5a,b, the APTES-SAM-modified silicon substrate is covered by GO or RGO sheets with disordered structures. The root-mean-square roughness/mean roughness for Figure 5a,b are 1.133/0.635 and 1.493/0.750 nm, respectively. As the section analysis indicates (Figure 5c,d), the thickness of the RGO sheet is ~1 nm. Such thickness is larger than the theoretical value of 0.34 nm for a perfectly flat sp^2-carbon-atom network[33,34] but is generally consistent with the value reported in previous studies.[7,33−35]

3.2. Adhesion and Microtribological Properties. It is believed that the adhesion force (F_{ad}) between an AFM tip and a sample surface includes the capillary force (F_C) as well as the solid−solid interactions, consisting of van der Waals force (F_{vdW}), electrostatic force (F_E), and chemical bonding force (F_B).[36,37] Therefore, F_{ad} can be expressed as

$$F_{ad} = F_C + F_{vdW} + F_E + F_B$$

where F_C is a main contributor to adhesion and closely related to surface wettability, which can be evaluated by WCA.[20] Table 1 shows that the hydroxylated silicon wafer and APTES-GO are

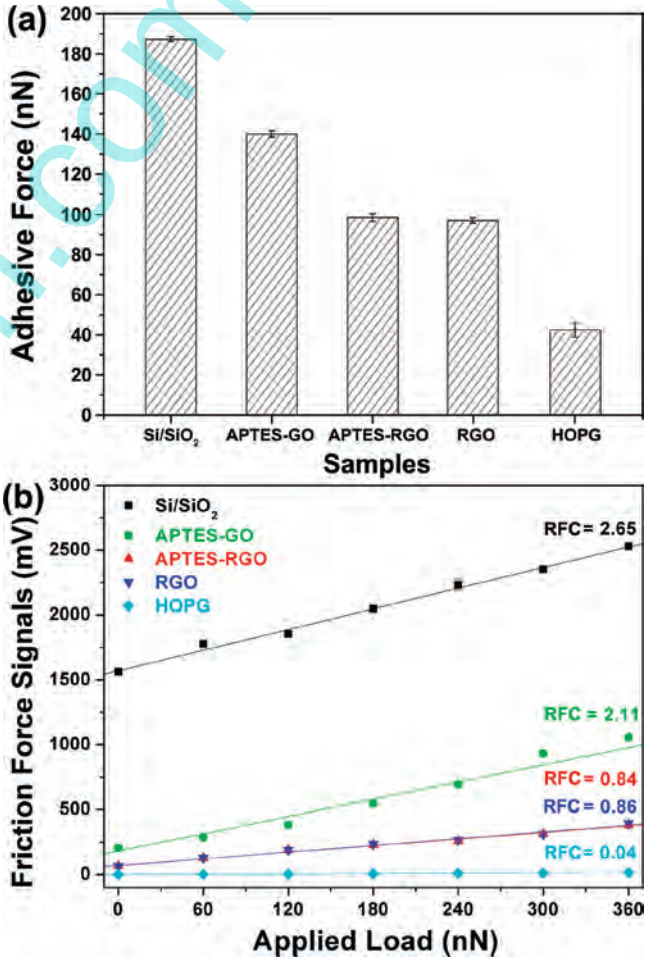

Figure 6. (a) Adhesion force and (b) friction-versus-load curves for different samples.

hydrophilic with WCA of ~0 and 40.2°, respectively. Correspondingly, high adhesive forces of ~190/~140 nN are generated between the AFM tip and the samples of hydroxylated silicon substrate/APTES-GO (Figure 6a). Once APTES-GO is reduced, WCA increases to 85.5°, and adhesive force decreases to ~100 nN, exhibiting good adhesion resistance. The F_{ad} of HOPG is much

(32) Zhou, Y.; Bao, Q.; Tang, L. A. L.; Zhong, Y.; Loh, K. P. *Chem. Mater.* **2009**, *21*, 2950–2956.
(33) Nemes-Incze, P.; Osvath, Z.; Kamaras, K.; Biro, L. P. *Carbon* **2008**, *46*, 1435–1442.
(34) Jung, I.; Dikin, D. A.; Piner, R. D.; Ruoff, R. S. *Nano Lett.* **2008**, *8*, 4283–4287.
(35) Shen, J. F.; Hu, Y. Z.; Li, C.; Qin, C.; Shi, M.; Ye, M. X. *Langmuir* **2009**, *25*, 6122–6128.
(36) Binggeli, M.; Mate, C. M. *Appl. Phys. Lett.* **1994**, *65*, 415–417.
(37) Xiao, X. D.; Qian, L. M. *Langmuir* **2000**, *16*, 8153–8158.

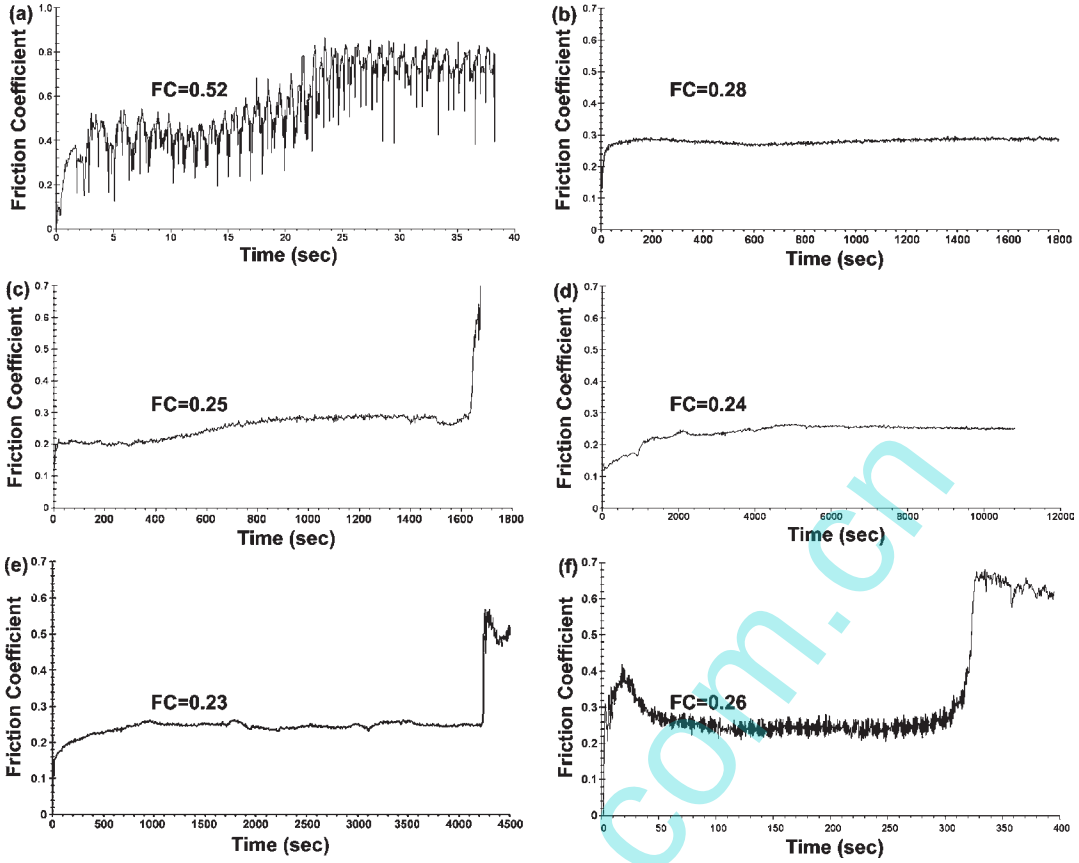

Figure 7. Variation in friction coefficient with time for various samples under different applied loads at sliding frequency of 1 Hz: (a) APTES-SAM, (b) graphite, (c) APTES-GO, (d) APTES-RGO, (e) RGO on bare Si substrate at an applied load of 0.1 N, and (f) APTES-RGO at an applied load of 0.2 N. The average friction coefficient (FC) was given above the corresponding curve.

lower than that of APTES-RGO, even though the difference in WCA between APTES-RGO and HOPG (~91°) is not prominent. This can be explained as follows: before being mounted to the AFM stage, both APTES-RGO and HOPG samples were exposed to air for several hours and days, and no net charges on their surfaces were expected to remain. Therefore, $F_E = 0$. F_B can also be neglected because the surfaces of the tip and samples are saturated with chemical bonds. Therefore, F_{ad} consists only of F_C and F_{vdW}. The difference in F_C between APTES-RGO and HOPG is presumed to be inapparent because of the small difference in WCA. Therefore, the relatively higher F_{ad} of APTES-RGO is most likely to be attributed to the higher F_{vdW}, which is supposed to be generated between the edges of RGO sheets and the AFM tip.[38] In other words, the large F_{vdW} may be a key factor in the relatively high adhesion of APTES-RGO.

The microtribological behavior of the fabricated samples in air was evaluated using an AFM. The measured friction forces versus applied loads are shown in Figure 6b. The friction forces are proportional to the applied loads, that is, obeying Amonton's Law

$$F_L = \mu F_N + F_0$$

where μ is the friction coefficient, F_L denotes the friction force, F_N is the normal load, and F_0 represents the friction force at an external load of zero.[39,40]

Precise real friction forces are difficult to obtain, and F_L is expressed as voltage signals; correspondingly, the real friction coefficients ($\mu = \partial F_L/\partial F_N$) could not be feasibly calculated. However, a relative friction coefficient (RFC), which is the slope of the force curve, can be obtained because the voltage signals are proportional to the strength of the real forces.[8] Therefore, for a given AFM probe, the RFCs for various samples can be compared among each other. Figure 6b shows that the hydroxylated silicon wafer possesses the highest friction and RFC. Both APTES-GO and APTES-RGO reduce friction. APTES-RGO exhibits the best lubricity, which can be assigned to the smallest adhesive force compared with the hydroxylated silicon wafer and APTES-GO (Figure 6a) as well as the lowest surface energy (reflected by the highest WCA of 85.5°).[18−20] However, the friction and RFC are still larger than those of HOPG. This may be ascribed to the relatively higher adhesion of APTES-RGO compared with that of HOPG. As shown in Figure 6, the adhesive force and microtribological difference between APTES-RGO and RGO on the bare silicon substrate are not prominent because of the identical surface structure and surface chemical composition reflected by the similar WCA of 85.5 and 82.4°.

3.3. Macrotribological Properties. The macrotribological behavior of the prepared film samples was tested on a ball-on-plate macrotribometer under different conditions. The results are shown in Figure 7. Figure 7a clearly shows that APTES-SAM displays poor tribological properties characterized by high friction and very short antiwear life (antiwear life refers to the sliding time at which friction coefficient rises sharply, corresponding to lubrication failure) under the testing conditions of 0.1 N and 1 Hz. Once GO is assembled, the sample exhibits improved tribological properties characterized by a reduced friction coefficient (~0.25) and a lengthened antiwear life (~1600 s, Figure 7c). Upon thermal

(38) Lee, H.; Lee, N.; Seo, Y.; Eom, J; Lee, S. *Nanotechnology* **2009**, *20*, 325701.
(39) Brewer, N. J.; Beaker, B. D.; Leggett, G. J. *Langmuir* **2001**, *17*, 1970–1974.
(40) Foster, T. T.; Alexander, M. R.; Leggett, G. J.; McAlpine, E. *Langmuir* **2006**, *22*, 9254–9259.

reduction, antiwear life increases further to > 10 800 s (Figure 7d). The vast improvement can be attributed to the deoxygenation of GO, which results in the low surface energy (reflected by high WCA) of the APTES-RGO sample. The RGO on the bare silicon substrate exhibits a wear life of ~4300 s (Figure 7e), suggesting that the RGO sheets possess good self-lubricating properties. Comparing the structure difference between APTES-RGO and RGO on the bare silicon substrate, the relatively long antiwear life of APTES-RGO may be ascribed to the covalent bonding of RGO to the silicon substrate mediated by APTES-SAM. However, under the conditions of 0.2 N and 1 Hz (Figure 7f), APTES-RGO shows a short lubricating life of ~300s. Therefore, the lubrication of APTES-RGO is more effective at relatively low applied loads. For comparison, the macrotribological properties of graphite plate (99%, obtained from Qingdao Hensen Graphite) were also studied (Figure 7b). However, the antiwear life was difficult to obtain within the limited testing period because of the considerable thickness, whereas the friction coefficient was measured to be 0.28, a little higher than that of APTES-RGO.

The tribological performance of another popular nanocarbon material, carbon nanotube (CNT), was also investigated in previous studies. Using AFM, Miyake[41] and Zhang[42] found that the vertically aligned CNT film possesses characteristics similar to APTES-RGO; that is, the friction and (relative) friction coefficient are higher than those of HOPG and lower than those of the silicon wafer. As to the macrotribological properties tested by a similar ball-on-disk tribometer, the friction coefficient is found to be ~0.3 to 0.5, which is clearly higher than that of GO/RGO.[43]

4. Conclusions

In this work, RGO sheets were covalently assembled onto a silicon surface via a multistep route. The microstructure and tribological properties of the samples were investigated. Results show that RGO exhibits excellent friction reduction and wear resistance properties under a low applied load, suggesting that APTES-RGO prepared by this method can serve as a low-friction antiwear coating in MEMS/NEMS. This simple strategy can be applied in many other substrates, such as glass, mica, and metal oxide, to assemble RGO. We anticipate that the assembly of RGO on silicon and other materials will provide promising applications in nanoelectronics, sensors, nanocomposites, batteries, supercapacitors, hydrogen storage, and so on.

Acknowledgment. We are grateful to the National Natural Science Foundation of China (grant nos. 20823008 and 50801065) and "Top Hundred Talents Program" of Chinese Academy of Sciences for financial support.

(41) Miyake, K.; Kusunoki, M.; Usami, H.; Umehara, N.; Sasaki, S. *Nano Lett.* **2007**, *7*, 3285–3289.
(42) Zhang, W.; Xu, B. S.; Tanaka, A.; Koga, Y. *Carbon* **2009**, *47*, 926–929.
(43) Hirata, A.; Yoshioka, N. *Tribol. Int.* **2004**, *37*, 893–898.